Chapter 3: Electrochemistry Using Self-Assembled DNA Monolayers on Highly Oriented Pyrolytic Graphite

Adapted from: Gorodetsky, A. A., Barton, J. K. (2006) *Langmuir 22*, 7917–7922.

ABSTRACT

Duplex DNA functionalized with pyrene has been utilized to fabricate DNA-modified electrodes on highly oriented pyrolytic graphite (HOPG). Films have been characterized using AFM and radioactive labeling as well as electrochemically. The data obtained are consistent with a close-packed structure in the film with helices oriented in a nearly upright orientation, as seen earlier with the fabrication of thiol-tethered duplexes on gold. Also as on gold, we observe the reduction of DNA-bound intercalators in a DNA-mediated reaction. The reduction of the intercalator is attenuated in the presence of the single-base mismatches, CA and GT, independent of the sequence composition of the oligonucleotide. This sensitivity to single-base mismatches is enhanced when methylene blue reduction is coupled in an electrocatalytic cycle with ferricyanide. The extended potential range afforded by the HOPG surface has allowed us also to investigate the electrochemistry of previously inaccessible metallointercalators, $Ru(bpy)_2dppz^{2+}$ and $Os(phen)_2dppz^{2+}$, at the DNA-modified HOPG surface. These results support the application of DNA-modified HOPG as a convenient and reproducible surface for electrochemical DNA sensors using DNA-mediated charge transport.

3.1 Introduction

Numerous studies have shown that DNA can efficiently transport charge in solution (1–6). Self-assembled DNA monolayers on gold have also been shown to mediate charge transport (CT) over significant distances (7–9). Either in solution or at a surface, DNA-mediated CT exhibits exquisite sensitivity to perturbations in base stacking as occur with single-base mismatches (10, 11), lesions (12, 13), and protein binding (14–17). Consequently, electrochemistry on DNA-modified electrodes has been useful in tools to detect DNA mutations, lesions, and protein/DNA interactions (5–7).

We have previously investigated the electrochemical properties of DNA monolayers assembled on gold (8, 9, 18–20). Electrochemical experiments have revealed that redox-active intercalators bound near the periphery of the film can serve as probes of DNA-mediated CT. The presence of even a single mismatch leads to dramatic attenuation of the electrochemical signal. This sensitivity to mutations within the base pair stack has been exploited for the detection of genomic sequence variations in a chip-based format (10).

The ability to manufacture DNA chips for large-scale mutational analysis has led us to investigate self-assembly of DNA monolayers at surfaces other than gold. Alternative surfaces may provide a route to disposable and inexpensive DNA chips with improved performance. We have chosen to focus our efforts on HOPG (highly oriented pyrolytic graphite) since this material provides a well-defined and clean surface possessing few defects (21).

Previous experiments with DNA on graphite have focused on the use of glassy carbon, pyrolytic graphite, and carbon paste electrodes. For example, Wang and co-workers have detected hybridization by electrochemical stripping of colloidal gold tags at screen-printed carbon paste electrodes (22–26). Additionally, Rusling and co-workers have detected both oxidative damage and nucleobase adducts using catalytic osmium and ruthenium square wave voltammetry (27–29). These methods have been applied to both DNA in solution and DNA immobilized at the electrode surface.

Pyrene modifications of both proteins and DNA have been made for surface functionalization of various graphite electrodes (30–33). For example, 1-pyrenebutyric acid *N*-hydroxysuccinimidyl ester has been utilized as a bifunctional reagent to immobilize a photosynthetic reaction center on pyrolytic graphite, and a cytochrome P450 mutant has been adsorbed onto a graphite surface via a pyrene-modified cysteine residue (30–32). Furthermore, proteins and oligonucleotides have been noncovalently attached to the graphitic side walls of carbon nanotubes via a pyrene moiety (33).

Utilizing this approach, we have synthesized oligonucleotides derivatized with pyrene for noncovalent immobilization of DNA duplexes on a graphitic surface. DNA sequences plus complements are prepared by standard solid-phase techniques with a pyrene moiety incorporated at the 5'-phosphate terminus. The pyrene-modified duplexes are then used to fabricate a DNA monolayer adsorbed onto HOPG. Using these films, we are able to detect single-base mismatches in oligonucleotides. DNA CT is mediated by the base pair stack on this surface.

3.2 Experimental Section

3.2.1 Materials

All reagents for DNA synthesis were purchased from Glen Research. Methylene blue, daunomycin, potassium ferricyanide, and all reagents used in the synthesis of pyrene-modified DNA were purchased from Sigma in the highest purity available and used as received. SPI-1 and SPI-3 grade HOPG was purchased from SPI, Inc. Buffers were prepared with Milli-Q water and filtered with a 0.2 μm filter.

3.2.2 Synthesis of DNA and Redox-Active Probes

Oligonucleotides were prepared using standard phosphoramidite chemistry on an Applied Biosystems 394 DNA synthesizer, purified by HPLC, and characterized by mass spectrometry. Pyrene-terminated oligonucleotides were synthesized in the following two ways: In the first strategy, oligonucleotides were prepared by solid-phase synthesis on a CPG resin with an unprotected hydroxyl group at the 5' terminus. The 5'-OH was treated with a 120 mg/mL solution of carbonyldiimidazole in dioxane for 90 min followed by an 80 mg/mL solution of 1,6-diaminohexane. For tether variations, ethylenediamine or 1,10-diaminononane was used instead. The free amine was then treated with 1-pyrenebutyric acid *N*-hydroxysuccinimidyl ester, leaving a pyrene moiety at the 5' terminus. In the second strategy, the free hydroxyl at the 5' terminus of the oligonucleotide was condensed with a 2-cyanoethyl *N*,*N*-diisopropylphosphoramidite of 1-pyrenebutanol on the DNA synthesizer. The phosphoramidite was prepared using a modified literature procedure (34). In brief, 500 mg of *N*,*N*-diisopropylethylamine was added to 5 mL of a 20 mg/mL solution of 1-pyrenebutanol in acetonitrile under an inert argon atmosphere.

While the reaction mixture was gently stirred, 90 mg of *N*,*N*-diisopropylphosphoramidochloridite was added dropwise. The reaction progress was monitored by TLC before the reaction mixture was moved to an extraction funnel and washed twice with 5% (by volume) $NaHCO_3$ and 3 M NaCl. The organic layer was collected, dried with Na_2SO_4, and rotovapped to a yellow oil. The phosphoramidite was dissolved in 1 mL of acetonitrile and used immediately for DNA synthesis.

The modified oligonucleotides were cleaved from the resin with concentrated ammonium hydroxide before being stringently purified by HPLC with a C18 column. Incorporation of the pyrene moiety was confirmed by HPLC retention times, UV-vis spectra, and MALDI-TOF mass spectrometry. Pyrene-modified single-strand DNA was hybridized with its complement by heating equimolar amounts of each strand (100 μM) in buffer, pH 7.1, containing 5 mM P_i and 50 mM NaCl to 90 º C followed by cooling to ambient temperature. Since single-stranded DNA can adsorb to graphite, great care was taken during quantification of DNA to ensure that equimolar amounts of each strand were annealed to form duplexes.

$[Ru(bpy)_2dppz]Cl_2$ and $[Os(phen)_2dppz]Cl_2$ (dppz = dipyridophenazine) were prepared and purified according to established protocols (33–38). Oligonucleotides and metallointercalators were quantified by UV-vis spectroscopy as previously described (4, 8, 9, 33–38).

3.2.3 Preparation of DNA-Modified Electrodes

Electrodes were constructed using a procedure modified from the literature (39). Briefly, a 10 mm × 10 mm × 1 mm HOPG block was affixed to a copper square with silver paste and mounted in a Teflon holder. The active area of this working electrode

was defined by a Viton or silicon O-ring mounted in a Teflon cap. To minimize mechanical stress on the HOPG block, electrical contact to the copper square was made with a spring-loaded pin. A clean and reproducible surface with few defects was crucial to the success of all electrochemistry experiments. Consequently, a fresh HOPG surface was cleaved with 3-M scotch tape before each experiment. The exposed surface was immediately used for electrochemistry experiments or immediately modified with DNA. Duplex DNA containing a pyrene moiety was deposited onto the HOPG surface in buffer, pH 7.1, containing 5 mM P_i 50 mM NaCl, and 100 mM $MgCl_2$; Mg^{2+} is included to ensure a closely packed film (8–11, 18–20). DNA films were allowed to form in a humidified chamber over a period of 4–24 hours.

3.2.4 Electrochemical Experiments

Cyclic voltammetry and chronocoulometry experiments were performed using a CH Instruments electrochemical analyzer (Austin, TX). Unless otherwise noted, experiments were performed at ambient temperature in buffer, pH 7.1, containing 5 mM P_i and 50 mM NaCl under an argon atmosphere. For daunomycin experiments, pH = 8. A custom-built three-compartment electrochemical cell was used for all experiments with a Pt auxiliary electrode, an SPI-1 grade HOPG working electrode, and a saturated calomel (SCE) or silver/silver chloride (Ag/AgCl) reference electrode. The compartment containing the reference electrode was separated from the rest of the cell with a Luggin capillary.

For metallointercalators, the redox potentials on bare HOPG are reported versus Ag/AgCl at a 500 mV/s scan rate for a freshly cleaved surface featuring some defects. The potentials of transition-metal complexes on HOPG have previously been shown to be

highly dependent on the defect density of the HOPG surface (21). Consequently, variations of ±50 mV were observed for cathodic peak potentials on bare HOPG.

3.2.5 Atomic Force Microscopy Experiments

All AFM measurements were performed using an MFP-3D atomic force microscope from Asylum Research, Inc. (Santa Barbara, CA). The HOPG block was mounted in a custom-designed glass chamber before being modified with DNA as described. AFM measurements were performed in buffer, pH 7.1, containing 5 mM P_i and 50 mM NaCl in either contact (constant force) or tapping mode. Commercially available silicon tips were utilized for all experiments.

3.2.6 Radioactive Labeling and Quantification

Before being hybridized to its pyrene-modified complements, the oligonucleotide was labeled at the 5' end with [gamma-^{32}P]ATP and polynucleotide kinase. A 0.25 cm^2 surface area was defined on an SPI-3 grade HOPG block and then modified with DNA as described. Samples were rinsed thoroughly and dried before being counted on an LS 5000TD scintillation counter (counts were adjusted for attenuation by the HOPG). Quantification was performed by comparing samples to calibration standards prepared from known quantities of labeled oligonucleotide.

3.3 Results and Discussion

3.3.1 Surface Characterization

After hybridization, densely packed DNA monolayers are self-assembled on a freshly cleaved HOPG surface with excess Mg^{2+} to permit close packing. Well-packed

films are crucial to the success of these experiments, so noncovalent intercalator binding is restricted to the upper segments of DNA. Thus, extensive characterization of the DNA monolayers is necessary. Quantitative characterization of the DNA-modified surface does reveal that the fabrication on HOPG resembles that found earlier on gold, as schematically illustrated in Figure 3.1 (40, 41).

AFM measurements were utilized to explore the morphology of DNA monolayers self-assembled on HOPG. Previous experiments on Au have focused on the effect of applied potential and linker structure on the morphology of 15-mer DNA films (40, 41). Additionally, AFM measurements on DNA films in solution have been used for label-free detection of hybridization (42, 43). In this work, we have chosen to examine the effect of sequence composition and duplex length on film formation at a HOPG surface. On the basis of AFM measurements, we find that duplexes of 10-, 14-, 15-, and 20-mer lengths form smooth, featureless films. Regardless of duplex length, these films appear to completely cover the HOPG surface.

To determine the film depth, a small patch of DNA may be removed from the HOPG surface by applying a vertical force with the AFM tip (40–43). Subsequent height contrast measurements between the resulting square and the surrounding covered surface are used to determine the film depth. AFM measurements for 14- and 15-mer sequences show film depths of 4.3 and 4.4 nm, respectively. The values found for 15-mer duplexes closely agree with previous experiments on Au, where a film depth of 4.5 nm was observed. In addition, height contrast measurements reveal that 10-mer duplexes result in shallower films whereas 20-mer duplexes result in deeper films. The observed thicknesses correspond to those expected for duplexes oriented at a ~ 45 º angle with

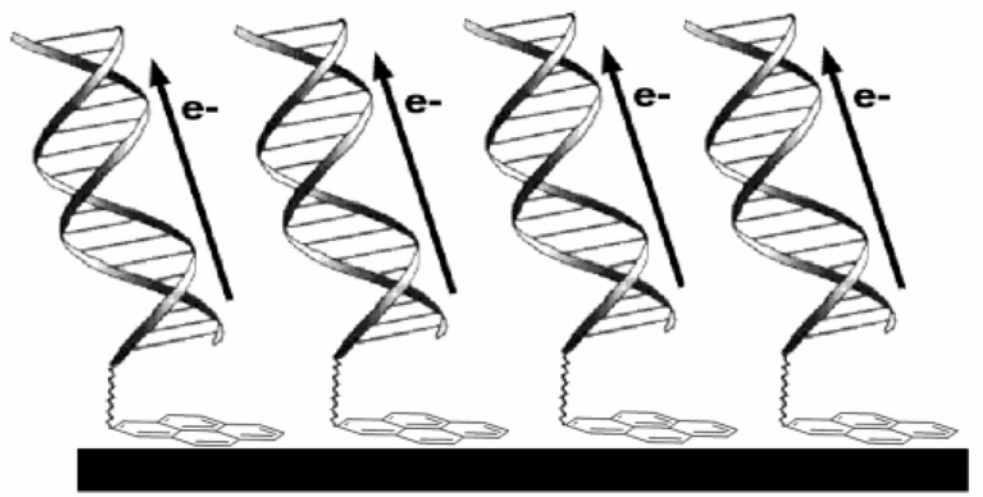

Figure 3.1: Schematic illustration of DNA duplexes modified with a pyrene moiety assembled on an HOPG surface. Surface characterization is consistent with DNA duplexes bound to HOPG in a nearly upright orientation and closely packed.

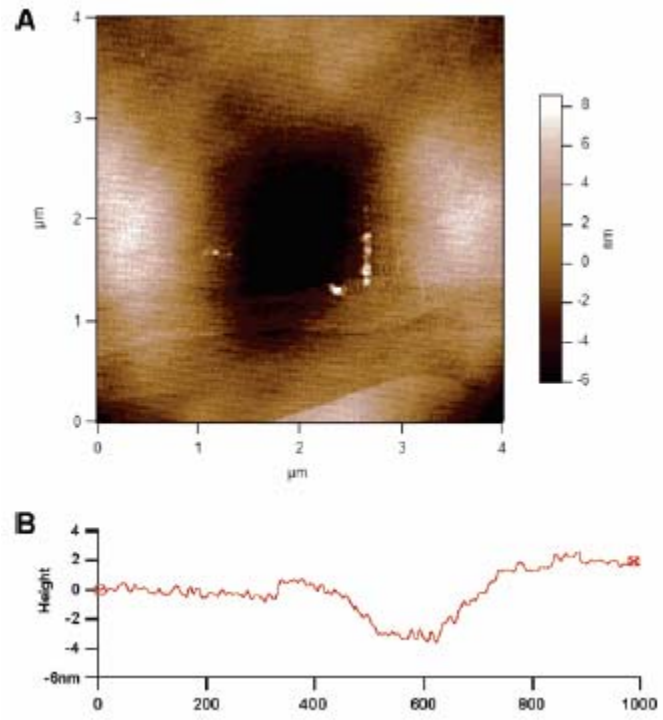

Figure 3.2: AFM characterization of DNA-modified HOPG: (A) typical AFM image of a patch of DNA removed from a monolayer of 20-mer duplexes on HOPG (tapping mode); (B) typical depth profile of a patch of DNA removed from a monolayer of 14-mer duplexes on HOPG (contact mode). All measurements were taken in buffer at pH 7.1, containing 5 mM P_i and 50 mM NaCl. Sequences were for (A) pyrene-$(CH_2)_3CONH(CH_2)_6NHCO$-5'-AGT ACA GAG TAC AGT ACG CG-3' plus complement and for (B) pyrene-$(CH_2)_3CONH(CH_2)_6NHCO$-5'-ATT ATA TAA TTG CT-3' plus complement.

respect to the surface assuming a fully extended alkane tether (40–43). A typical film with a DNA patch removed and a typical height profile are shown in Figure 3.2.

Surface coverage is also quantitated by radioactive labeling. Here, on HOPG, we find a DNA duplex coverage of 47 ± 18 pmol/cm^2; this corresponds to a fractional surface coverage of 85%, which corresponds to close packing of DNA duplexes oriented at ~ 45 º. Previous radioactive labeling experiments on Au found a surface coverage of 41 pmol/cm^2, corresponding to a fractional surface coverage of 75% (8–11, 18–20). The intrinsically flat HOPG surface (relative to gold) may allow for slightly denser films corresponding to the higher observed surface coverage. Additionally, the flat "footprint" attachment of the pyrene may aid in close packing.

Quantitation of surface coverage may also be performed electrochemically. Assay using ruthenium hexammine (42–44) yields coverages similar to those found by radioactive labeling and AFM, a value of 44.6 ± 14 pmol/cm^2. It should be noted that, as a companion to all experiments, films are routinely screened using ferricyanide as an anionic probe. At a close-packed DNA-modified surface, ferricyanide remains electrochemically silent, consistent with complete coverage (8–11, 18–20).

These results therefore all are consistent with results seen earlier on Au. Fabrication of DNA duplexes on HOPG with high concentrations of Mg^{2+} leads to closely packed helices arranged at a ~ 45 º angle in the absence of an applied potential.

3.3.2 Electrochemistry at a DNA-Modified HOPG Surface

Shown in Figure 3.3 is the cyclic voltammetry for methylene blue (MB) on bare HOPG and HOPG modified with duplex DNA featuring a pyrene moiety. At the DNA-modified surface, MB shows a redox couple at -280 mV versus Ag/AgCl, shifted by 30 mV from

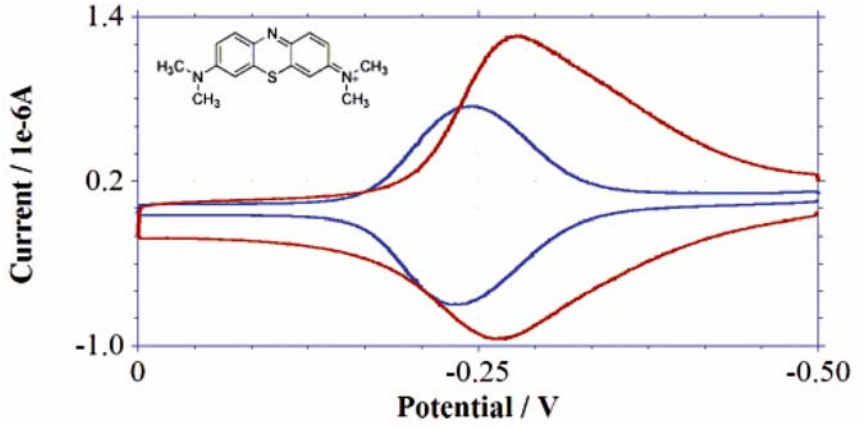

Figure 3.3: Cyclic voltammetry of 0.5 µM methylene blue at a 100 mV/s scan rate with a 0.18 cm^2 working area in buffer, pH 7.1, containing 5 mM P_i and 50 mM NaCl. Cyclic voltammograms are shown versus Ag/AgCl for a bare electrode in blue and a DNA-modified electrode in red. The sequence was pyrene-$(CH_2)_4P_i$-5'-AGT ACA GTC ATC GCG-3'.

that found on bare HOPG. A similar shift is observed for MB bound to DNA on Au (18–20). Since aromatic molecules tightly adsorb onto bare pyrolytic graphite, the electrochemistry of MB on both DNA-modified and bare HOPG surfaces leads to linear plots of peak current as a function of scan rate, although with different slopes; the redox-active species is surface-bound in both cases (45). It should also be noted that control experiments with MB on HOPG surfaces using DNA duplexes lacking the pyrene moiety yield broadened and irreproducible electrochemical signals. This is most likely due to the disordered orientation of duplexes lacking a pyrene moiety on the HOPG surface.

We also examined a range of tether lengths for the pyrene linked to DNA in these studies. In earlier studies of daunomycin covalently bound to thiolated DNA on Au, we found that electron-transfer rates were limited by tunneling through the alkanethiol tether (46). Here different tether lengths have been explored in studies using noncovalent MB; because the noncovalent MB may bind to several sites near the top of the film, detailed information concerning rates as a function of distance can therefore not be obtained. Instead we were interested in determining the optimum length for close packing of the film and reproducible electrochemistry. Good reproducibility is in fact found with tethers $(CH_2)_4P_i$, $(CH_2)_3CONH(CH_2)_2NHCO$, $(CH_2)_3CONH(CH_2)_6NHCO$, and $(CH_2)_3CONH(CH_2)_{10}NHCO$. For all of these linkers, larger peak splittings between cathodic and anodic waves are evident in comparison to those for bare HOPG (15 mV versus 5 mV for MB in Figure 3.3). Extending the length of the tether between the pyrene and the duplex leads to even greater peak splittings at these scan rates, a result which is consistent with electron-transfer rates being limited by tether length. For example, cyclic voltammograms at pyrene-$(CH_2)_3CONH(CH_2)_2NHCO$-DNA-modified surfaces exhibit a

peak splitting of 23 ± 7 mV for MB, while surfaces modified with pyrene-$(CH_2)_3CONH(CH_2)_{10}NHCO$-DNA exhibit a peak splitting of 52 ± 10 mV for MB. These observations are consistent with the structural model for the DNA film shown in Figure 3.1 where the tether intervenes between the pyrene bound to HOPG and the DNA duplex.

3.3.3 Electrochemistry on HOPG Is DNA-Mediated

If CT is DNA-mediated, the introduction of a mismatch within the base pair stack should lead to a significant attenuation of the electrochemical signal at the DNA film; we have found in a range of experiments that the perturbation in the base pair stack associated with a mismatch inhibits CT (1–4, 8–11). We find that electrochemistry on DNA-modified HOPG with either daunomycin or MB as the redox-active probe leads to a significant diminution in the integrated cathodic charge (Q_c) for fully base paired (WT) and mismatch-containing (MM) DNA films. For the duplex sequence pyrene-$(CH_2)_4P_i$-5'-AGT ACA GT*C* ATC GCG-3', Q_{MM}/Q_{WT} = 0.51 with daunomycin as the redox probe and Q_{MM}/Q_{WT} = 0.41 for MB, where the italicized base indicates the position of a CA mismatch.

We also examined the electrochemistry using DNA duplexes of different sequences. As evident in Figure 3.4 and as previously shown for DNA monolayers on gold, mismatch detection is independent of sequence context (8, 9). In particular, AT-rich sequences yield results equivalent to those of sequences rich in GC content. The sequence pyrene-$(CH_2)_3CONH(CH_2)_6NHCO$-5'-ATT ATA TAA TTG CT-3' gives Q_{MM}/Q_{WT} = 0.60 with daunomycin as the redox probe and Q_{MM}/Q_{WT} = 0.46 for MB. The observed variations in Q_{MM} and Q_{WT} with daunomycin and MB between various sequences and linker lengths are well within experimental error.

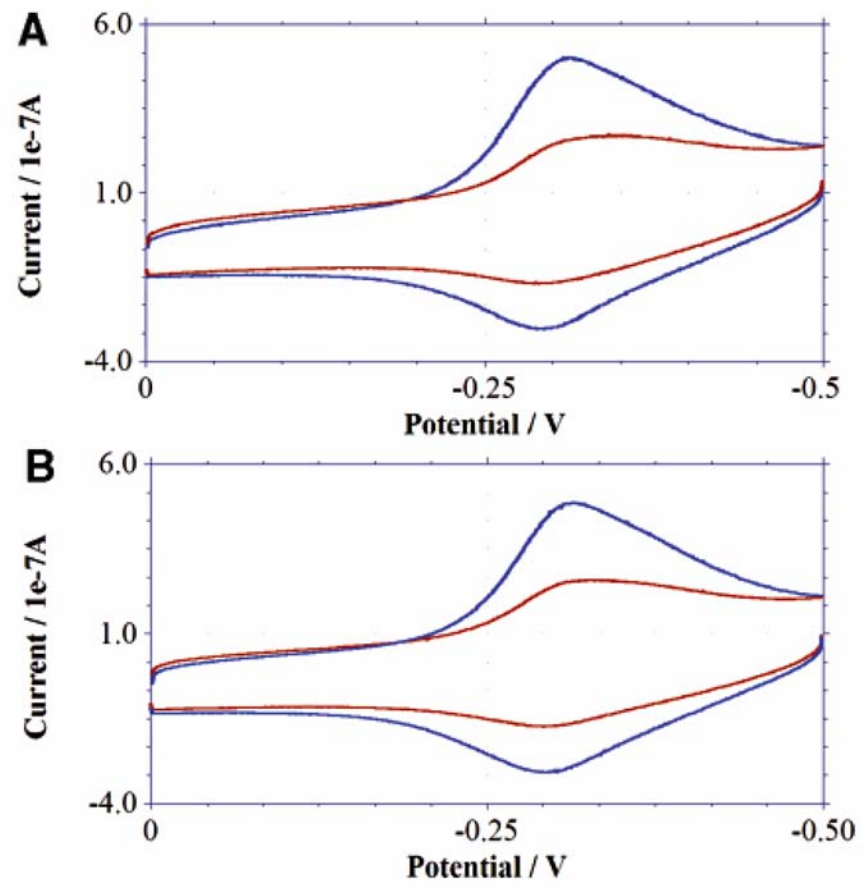

Figure 3.4: Cyclic voltammetry of 0.5 µM methylene blue at a 100 mV/s scan rate versus SCE in a buffer, pH 7.1, containing 5 mM P_i and 50 mM NaCl for an electrode modified with fully base paired DNA duplexes in blue and an electrode modified with duplexes featuring a CA mismatch in red. Sequences were for (A) pyrene-$(CH_2)_3CONH(CH_2)_6NHCO$-5'-AGT ACA GT*C* ATC GCG-3' and for (B) pyrene-$(CH_2)_3CONH(CH_2)_6NHCO$-5'-ATT ATA TA*A* TTG CT-3', where the italicized base indicates the position of the CA mismatch.

Coupling MB to an electrocatalytic cycle involving ferricyanide allows for even greater discrimination between fully base paired and mismatch-containing DNA films (10, 11). Figure 3.5 shows cyclic voltammetry for 0.5 μM MB in the presence of 2 mM ferricyanide on HOPG with pyrene-tethered duplex DNA with and without a CA or GT mismatch. Without the mismatch, a highly asymmetric cyclic voltammogram is evident, consistent with electrocatalytic behavior (45, 47–49). As expected for an electrocatalytic process, the E_p of the electrocatalytic peak matches the $E_{1/2}$ of the MB peak at a DNA-modified surface without $K_3Fe(CN)_6$ (45, 47–49). Moreover, note the complete absence of a ferricyanide signal due to repulsion of the anionically charged probe by the DNA monolayer.

Greater sensitivity in discriminating the single-base mismatch is obtained via electrocatalysis. We can, for example, easily detect the thermodynamically stable GT wobble base pair (Figure 3.5). Chronocoulometry using a -350 mV step with ferricyanide and MB gave an integrated charge of 111.5 ± 12.0 μC for fully base paired DNA compared to maximal charges at 5 s of 49.5 ± 8.1 and 55.4 ± 20.3 for duplexes featuring a CA or GT mismatch, respectively. These results underscore that mismatch discrimination depends on CT through the base pair stack rather than on thermodynamic differences associated with hybridization events.

Results for different tethers and different sequences, with and without electrocatalysis, are summarized in Table 3.1. Significantly, these results, taken together, all fully support the conclusion that CT on HOPG modified with pyrene-tethered DNA is DNA-mediated. The results found here for HOPG compare closely to those found for DNA films fabricated on Au.

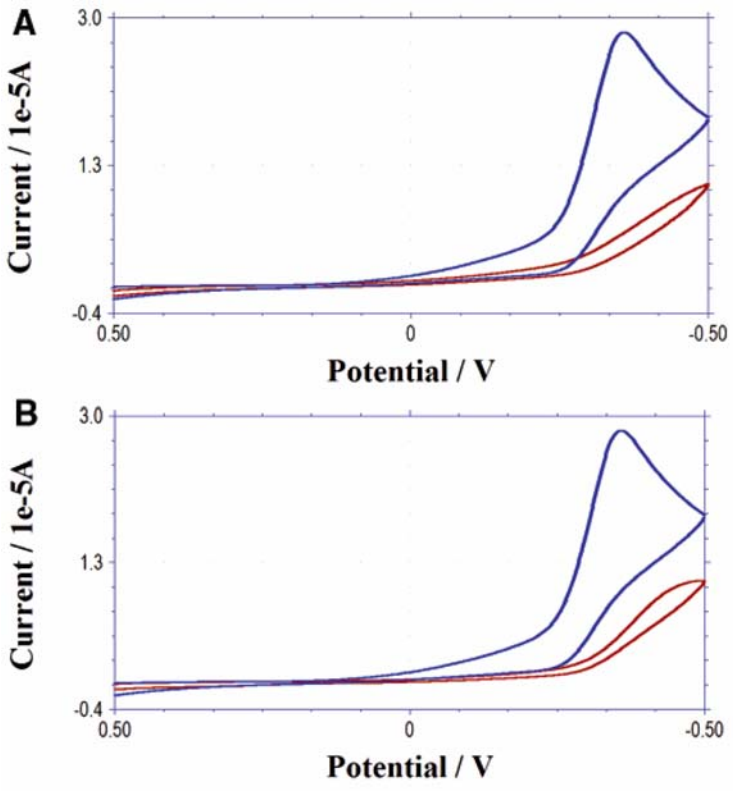

Figure 3.5: Cyclic voltammetry of 0.5 µM methylene blue and 2 mM $K_3Fe(CN)_6$ at a 100 mV/s scan rate versus SCE in buffer, pH 7.1, containing 5 mM P_i and 50 mM NaCl for an electrode modified with fully base paired DNA duplexes in blue and an electrode modified with duplexes featuring a mismatch in red. Sequences utilized were for (A) pyrene-$(CH_2)_3$CONH$(CH_2)_6$NHCO-5'-AGT ACA G*T*C ATC GCG-3' and for (B) pyrene-$(CH_2)_3$CONH$(CH_2)_6$NHCO-5'- AGT ACA GT*C* ATC GCG-3', where the italicized base indicates the position of the GT or CA mismatch, respectively.

Table 1. Summary of Mismatch Detection with Various Linkers on DNA-Modified HOPG Electrodes

duplex[a]	linker	I_{pc}[b] (μA)	I_{pc}[c] (μA)
wild type	$(CH_2)_3CONH(CH_2)_2NHCO$	0.22 (0.04)	15.6 (2.0)
CA mismatch	$(CH_2)_3CONH(CH_2)_2NHCO$	0.12 (0.02)	7.1 (2.0)
wild type	$(CH_2)_3CONH(CH_2)_6NHCO$	0.15 (0.01)	14.2 (1.9)
CA mismatch	$(CH_2)_3CONH(CH_2)_6NHCO$	0.10 (0.02)	4.5 (3.6)
GT mismatch	$(CH_2)_3CONH(CH_2)_6NHCO$	0.10 (0.03)	4.6 (3.6)
wild type	$(CH_2)_3CONH(CH_2)_{10}NHCO$	0.27 (0.13)	12.4 (4.0)
CA mismatch	$(CH_2)_3CONH(CH_2)_{10}NHCO$	0.06 (0.12)	3.2 (1.7)
wild type	$(CH_2)_4P_i$	0.22 (0.10)	15.9 (4.4)
CA mismatch	$(CH_2)_4P_i$	0.09 (0.04)	4.8 (2.3)

[a] Duplexes of the type pyrene-linker-5′-AGT ACA GTC ATC GCG-3′ plus complement where wild type indicates that the duplex is fully base paired. [b] Peak current, with 0.5 μM methylene blue. [c] Peak current with electrocatalysis, with 0.5 μM methylene blue and 2 mM potassium ferricyanide. Standard deviations are in parentheses.

Table 3.1: Summary of mismatch detection with various linkers on DNA-modified HOPG electrodes.

3.3.4 DNA Electrochemistry with Various Intercalators

Electrochemistry with DNA films on HOPG affords an extended potential range compared to that for thiolated DNA monolayers on gold (18–20, 50, 51). Thus, exploiting this characteristic, DNA films were investigated using $Ru(bpy)_2dppz^{2+}$ and $Os(phen)_2dppz^{2+}$ as intercalating redox-active probes (Figure 3.6). These metallointercalators exhibit redox couples at the edge of the potential window of Au, with larger applied biases leading to thiol desorption (50, 51). The extended potential range on HOPG allows us also to test the electrochemical activity of DNA-bound $Ru(bpy)_2dppz^{2+}$ and $Os(phen)_2dppz^{2+}$, two well-characterized metallointercalators (35–38). Surface-bound $Ru(bpy)_2dppz^{2+}$ and $Os(phen)_2dppz^{2+}$ display quasi-irreversible redox couples at the DNA-modified surface, which can be assigned to reduction of the dppz ligand (35–38). Moreover, all of these intercalators bound to the DNA-modified electrodes exhibit linear plots of peak current as a function of scan rate, as expected for surface-bound species.

Mismatch detection is also possible with metallointercalators bound to DNA at the HOPG surface (Figure 3.7). When DNA films containing a CA mismatch are electrochemically interrogated with $Os(phen)_2dppz^{2+}$, a significant diminution compared to fully matched DNA films in both the cathodic and anodic waves is observed. This result provides further evidence that charge transfer to the metallointercalators is in fact also DNA-mediated on HOPG.

Suprisingly, electrocatalytic activity for $Os(phen)_2dppz^{2+}$ is evident in conjunction with ferricyanide, yielding amplification of the DNA-mediated electrochemical signal.

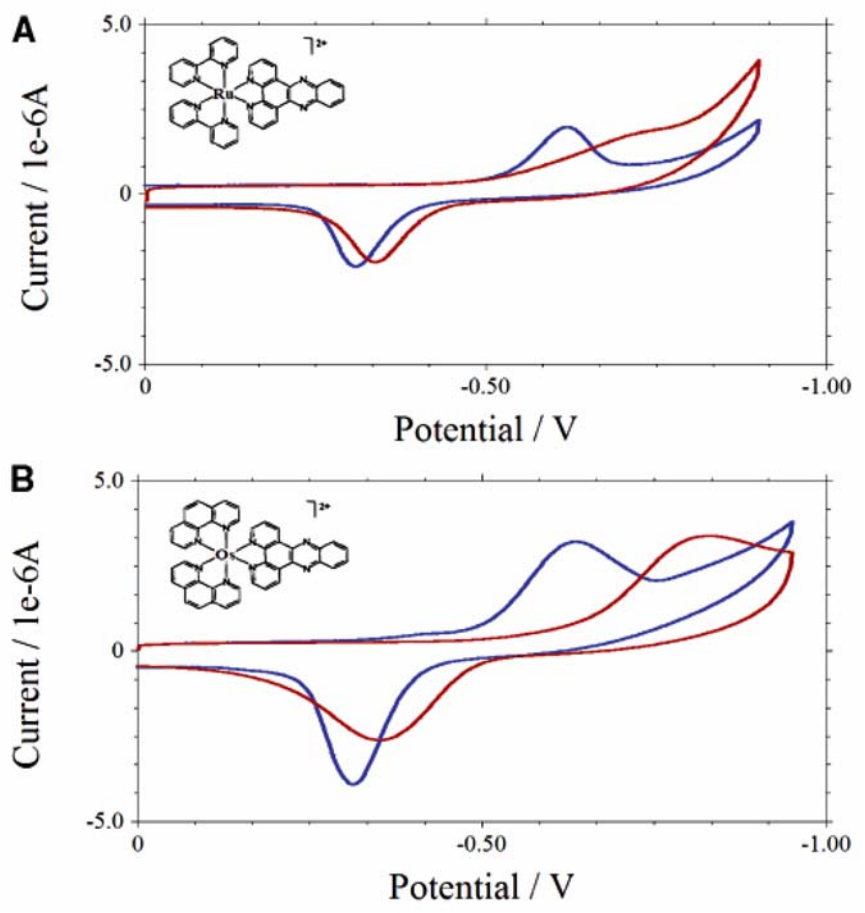

Figure 3.6: Cyclic voltammetry versus Ag/AgCl for electrodes modified with fully base paired duplexes at a 500 mV/s scan rate in buffer, pH 7.1, containing 5 mM P_i and 50 mM NaCl. Bare electrodes are in blue, and DNA-modified electrodes are in red for (A) 2 µM $Ru(bpy)_2dppz^{2+}$ and (B) 2 µM $Os(phen)_2dppz^{2+}$. The sequence was pyrene-$(CH_2)_4P_i$-5'-AGT ACA GTC ATC GCG-3'.

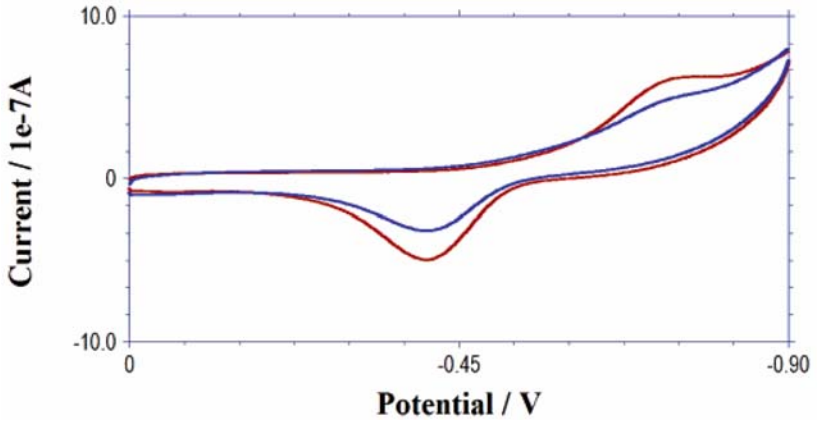

Figure 3.7: Cyclic voltammetry of 2 µM $Os(phen)_2dppz^{2+}$ at a 100 mV/s scan rate versus SCE in a buffer, pH 7.1, containing 5 mM P_i and 50 mM NaCl. The electrode modified with fully base paired DNA duplexes is in blue, and the electrode modified with duplexes featuring a CA mismatch is in red. The sequence was pyrene-$(CH_2)_3CONH(CH_2)_6NHCO$-5'-AGT ACA GT*C* ATC GCG-3', where the italicized base indicates the position of the CA mismatch.

It is noteworthy, however, that secondary peaks were observed to grow in after repeated cycling of the Ru or Os intercalators at the DNA-modified electrodes; this may indicate some decomposition of the DNA-bound metallointercalators upon reduction of the dppz ligand. Nonetheless, in sum, these data, with and without electrocatalysis, certainly indicate that HOPG surfaces offer an opportunity to explore the rich electrochemistry of this family of metallointercalators bound to DNA.

3.4 Implications

DNA-mediated electrochemistry provides a convenient route to the detection of perturbations within the base pair stack. Electrochemical detection avoids expensive equipment associated with fluorescence measurements and radioactive labeling. Additionally, stringent hybridization conditions are not necessary, and the electrochemical signal can be easily amplified via electrocatalysis. Here we establish this same DNA-mediated electrochemistry at a graphite surface. The methodology developed here provides a convenient strategy to fabricate electroactive DNA chips on graphite. Moreover, the extended potential range on HOPG allows us to probe and exploit previously inaccessible redox-active species bound to DNA.

REFERENCES

(1) Boon, E. M., Barton, J. K. (2002) *Curr. Opin. Struct. Biol. 12*, 320–329.

(2) O'Neill, M. A.; Barton, J. K. (2004) *Topics in Current Chemistry: Electron Transfer in DNA I* (G. B. Schuster), pp. 67–115, Springer-Verlag, New York.

(3) O'Neill, M. A., Barton, J. K. (2005) *Charge Transfer in DNA: From Mechanism to Application* (H.-A. Wagenknecht), pp. 27–75, Wiley-VCH, Hoboken.

(4) Delaney, S., Barton, J. K. (2003) *J. Org. Chem. 68*, 6475–6483.

(5) Giese, B. (2000) *Acc. Chem. Res. 33*, 631–636.

(6) Schuster, G. B. (2000) *Acc. Chem. Res. 33*, 253–260.

(7) Drummond, T. G., Hill, M. G., Barton, J. K. (2003) *Nat. Biotechnol. 21*, 1192–1199.

(8) Kelley, S. O.; Jackson, N. M.; Hill, M. G.; Barton, J. K. (1999) *Angew. Chem., Int. Ed. 38*, 941–945.

(9) Liu, T., Barton, J. K. (2005) *J. Am. Chem. Soc. 127*, 10160–10161.

(10) Boon, E. M., Ceres, D. M., Drummond, T. G., Hill, M. G., Barton, J. K. (2000) *Nat. Biotechnol. 18*, 1096–1100.

(11) Kelley, S. O., Boon, E. M., Barton, J. K., Jackson, N. M., Hill, M. G. (1999) *Nucleic Acids Res. 27*, 4830–4837.

(12) Boal, A. K., Barton, J. K. (2005) *Bioconjugate Chem. 16*, 312–321.

(13) Boon, E. M., Barton, J. K., Pradeepkumar, P. I., Isaksson, J., Petit, C. Chattopadhyaya, J. (2002) *Angew. Chem., Int. Ed. 41*, 3402–3405.

(14) Boon, E. M., Salas, J. E., Barton, J. K. (2002) *Nat. Biotechnol. 20*, 282–286.

(15) Boon, E. M., Livingston, A. L., Chmiel, N. H., David, S. S., Barton, J. K. (2003) *Proc. Natl. Acad. Sci. U.S.A. 100*, 12543–12547.

(16) DeRosa, M. C., Sancar, A., Barton, J. K. (2005) *Proc. Natl. Acad. Sci. U.S.A. 102*, 10788–10792.

(17) Boal, A. K., Yavin, E., Lukianova, O. A., O'Shea, V. L., David, S. S., Barton, J. K. (2005) *Biochemistry 44*, 8397–8407.

(18) Kelley, S. O., Jackson, N. M., Hill, M. G., Barton, J. K. (1997) *Bioconjugate Chem. 8*, 31–37.

(19) Boon, E. M., Barton, J. K. (2003) *Bioconjugate Chem. 14*, 1140–1147.

(20) Boon, E. M., Jackson, N. M., Wightman, M. D., Kelley, S. O., Barton, J. K., Hill, M. G. (2003) *J. Phys. Chem. B 107*, 11805–11812.

(21) McCreery, R. L. (1990) *Electroanalytical Chemistry* (A. J. Bard,), pp. 221– Marcel Dekker, New York.

(22) Palecek, E., Jelen, F., Teijeiro, C., Fucik, V., Jovin, T. M. (1993) *Anal. Chim. Acta 273*, 175–186.

(23) Wang, J., Palecek, E., Nielsen, P. E., Rivas, G., Cai, X., Shiraishi, H., Dontha, N., Luo, D., Farias, P. A. M. (1996) *J. Am. Chem. Soc. 118*, 7667–7670.

(24) Wang, J., Xu, D., Kawde, A., Polsky, R. (2001) *Anal. Chem. 73*, 5576–5581.

(25) Wang, J. (2002) *Anal. Chim. Acta 469*, 63–71.

(26) Wang, J., Liu, G., Jan, M. R. (2004) *J. Am. Chem. Soc. 126*, 3010–3011.

(27) Zhou, L., Rusling, J. F. (2001) *Anal. Chem. 73*, 4780–4786.

(28) Mugweru, A., Wang, B., Rusling, J. F. (2004) *Anal. Chem. 76*, 5557–5563.

(29) Dennany, L., Forster, R. J., White, B., Smyth, M., Rusling, J. F. (2004) *J. Am. Chem. Soc. 126*, 8835–8841.

(30) Willner, I., Katz, E. (2000) *Angew. Chem., Int. Ed. 39*, 1180–1218.

(31) Katz, E. (1994) *J. Electroanal. Chem. 365*, 157–164.

(32) Udit, A. K., Hill, M. G., Bittner, V. G., Arnold, F. H., Gray, H. B. (2004) *J. Am. Chem. Soc. 126*, 10218–10219.

(33) Taft, B. J., Lazareck, A. D., Withey, G. D., Yin, A., Xu, J. M., Kelley, S. O. (2004) *J. Am. Chem. Soc. 126*, 12750–12751.

(34) Mann, J. S., Shibata, Y., Meehan, T. (1992) *Bioconjugate Chem. 3*, 554–558.

(35) Freidman, A. E., Chambron, J. C., Sauvage, J. P., Turro, N. J., Barton, J. K. (1990) *J. Am. Chem. Soc. 112*, 4960–4962.

(36) Delaney, S., Pascaly, M., Bhattacharya, P. K., Han, K., Barton, J. K. (2002) *Inorg. Chem. 41*, 1966–1974.

(37) Holmlin, R. E., Barton, J. K. (1995) *Inorg. Chem. 34*, 7–8.

(38) Holmlin, R. E., Yao, J. A. Barton, J. K. (1999) *Inorg. Chem. 38*, 174–189.

(39) Bowler, R., Davies, T. J., Hyde, M. E., Compton, R. G. (2005) *Anal. Chem. 77*, 1916–1919.

(40) Sam, M., Boon, E. M., Barton, J. K., Hill, M. G., Spain, E. M. (2001) *Langmuir 17*, 5727–5730.

(41) Kelley, S. O., Barton, J. K., Jackson, N. M., McPherson, L. D., Potter, A. B., Spain, E. M., Allen, M. J., Hill, M. G. (1998) *Langmuir 14*, 6781–6784.

(42) Zhou, D., Sinniah, K., Abell, C., Rayment. T. (2002) *Langmuir 18*, 8278–8281.

(43) Zhou, D., Sinniah, K., Abell, C., Rayment, T. (2003) *Angew. Chem. 42*, 4934–4397.

(44) Steel, A. B., Herne, T. M., Tarlov, M. J. (1998) *Anal. Chem. 70*, 4670–4677.

(45) Bard, A. J., Faulkner, L. R. (2001) *Electrochemical Methods, 2nd ed.*, John Wiley & Sons: New York.

(46) Drummond, T. G., Hill, M. G., Barton, J. K. (2004) *J. Am. Chem. Soc. 126*, 15010–15011.

(47) Boon, E. M., Barton, J. K., Bhagat, V., Nersissian, M., Wang, W., Hill, M. G. (2003) *Langmuir 19*, 9255–9259.

(48) Anson, F. C. (1980) *J. Phys. Chem. 84*, 3336–3338.

(49) Oyama, N., Anson, F. C. (1980) *Anal. Chem. 52*, 1192–1198.

(50) Wackerbarth, H., Grubb, M., Zhang, J., Hansen, A. G., Ulstrup, J. (2004) *Langmuir 20*, 1647–1655.

(51) Love, J. C., Estroff, L. A., Kriebel, J. K., Nuzzo, R. G., Whitesides, G. M. (2005) *Chem. Rev. 105*, 1103–1169.